Enhanced strain and stiffness evaluation of virgin and recycled single carbon fibres by means of one-dimensional digital image correlation

OPEN ACCESS
IOP Publishing
Made open access 1 May 2020
Measurement Science and Technology
Meas. Sci. Technol. **30** (2019) 035201 (12pp)
https://doi.org/10.1088/1361-6501/aafcad

Enhanced strain and stiffness evaluation of virgin and recycled single carbon fibres by means of one-dimensional digital image correlation

Jonas Huether, Daniel Esse, Peter Rupp, Michael Seitz and Kay André Weidenmann

Institute for Applied Materials, Karlsruhe Institute of Technology, Kaiserstr. 12, 76131 Karlsruhe, Germany

E-mail: Jonas.Huether@kit.edu

Received 16 August 2018, revised 3 December 2018
Accepted for publication 7 January 2019
Published 7 February 2019

Abstract

The Young's modulus of single carbon fibres, virgin and recycled, is investigated in this study. Single fibre measurements are enhanced in two fields: firstly, the cross-sectional area is calculated by taking individual measurements with a laser diffraction sensor and applying a sinusoidal fit to account for irregular fibre shapes. Secondly, strains during the loading cycle are measured directly by applying fluorescing tracking markers on the fibre and using one-dimensional digital image correlation. Several markers are applied on each side of the fibre to allow for a statistically verified evaluation. To achieve high-resolution images, a step-wise load cycle is applied. The load is increased in steps of 250 MPa until final failure. It is demonstrated that direct strain measurement and enhanced determination of the Young's modulus are possible for carbon fibres. It was further shown that the recycling of the carbon fibre by pyrolysis reduced the Young's modulus by approximately 10% compared to virgin fibres.

Keywords: single fibre test, SiFiT, digital image correlation, high tenacity carbon fibres, recycled carbon fibres, cross-sectional area

(Some figures may appear in colour only in the online journal)

1. Motivation and introduction

In recent years, recycling is starting to push into the field of composites due to tightened regulations and a general need for more sustainable materials [1]. However, recycling of composites is challenging as the interface between fibre and matrix has to be disintegrated to separate both components. This does directly contradict the goal of engineers to optimise the interface during the primary production routes. Various methods to disintegrate matrix and fibre are being researched nowadays but in regard of thermosets reinforced with carbon fibres, only pyrolysis processes are market-ready [2, 3]. As carbon fibres are by far more valuable than standard resins [4], the thermoset resin is pyrolysed in an inert atmosphere, leaving behind the carbon fibres. The carbon fibres can then be reprocessed with a new matrix. Consequently, designers and engineers are in need of accurate material data of the recycled fibres. Particularly, it has to be proven that despite the harsh conditions during the pyrolysis (temperature, pressure, etc) the fibre properties are not impaired.

Given the definition of the Young's modulus, $E = \frac{\sigma}{\epsilon} = \frac{F/A}{\epsilon}$, it is evident that in order to accurately determine the Young's modulus of single carbon fibres, the cross-sectional area A and the elongation ϵ of the fibre have to be measured as precisely as possible. The work at hand aims at improving the

measurement of both parameters and to adapt it to the conditions of single fibres. Two optical techniques will be used to measure strains and cross-sectional areas separately: strains will be measured by one-dimensional (1D) digital image correlation on marker beads applied to the fibre; cross-sectional areas will be determined by laser diffraction techniques in combination with mathematically fitting readings to approximate an oval shape.

In order to demonstrate the need for improved measurement methods, this paragraph is dedicated to the particularities of single fibres and the corresponding state-of-the-art in technology. The measurement of the cross-sectional area of carbon fibres is challenging due to the small diameter and deviations of the cross-section from a circular shape, as the fibre geometry depends on the type and production route. For instance, kidney-shaped and oval cross-sectional areas have been reported by Endo *et al*, Chae *et al* and Naito *et al* [5–7]. Hughes [8] displayed four typical tracings from SEM micrographs. His work shows both the non-circular cross-sectional area of carbon fibres and the uneven surface structure. A very distinct kidney-shaped cross-section of fibres can be found in Kumar *et al* and Marcuzzo *et al* [9, 10]. Additional information is found in Chand's 'Review of carbon fibres for composites' [11].

ASTM standard C1557-14 offers general ideas how to determine the cross-sectional area of carbon fibres and discusses their disadvantages. Metallographic preparations including optical inspections and laser diffractometry are recommended, but for the latter no formulas are given to account for non-circular shapes. In this regard, the work at hand will provide an approach to mathematically account for irregularities in the cross-sectional shape.

Furthermore, vibroscopic procedures to measure the linear density of fibres or cords instead of the cross-sectional area are reported in the literature. This alternative to diameter and cross-sectional determinations is introduced in [12] stating the basic physical context that the lowest natural frequency f_0 is related to the cross-sectional area A by

$$f_0 = \frac{1}{2l} \cdot \sqrt{\frac{T}{\rho \cdot A}} \tag{1}$$

with ρ being the density of the material, l the clamping length and T a force applied on the system [12]. The vibroscopic method is summarised in [13], emphasising the fact that the theory has been developed for uniform and circular strings. Titze and Hunter express doubts about neglecting the true cross-sectional area. In vocal ligaments they found a distinct influence of non-uniform cross-sectional areas upon the normal mode frequency of the vibrating system [14]. Taking into account the shape of carbon fibres, results for area determination should be evaluated with caution. Furthermore, the method is reliant upon the density of the fibres, and special attention must be given to a correct determination of the density, in particular for recycled fibres. Nonetheless, the method is frequently used prior to running tensile tests, but additional information about the reliability for non-circular fibres is not always presented [6, 15]. Indirect determination of the fibre diameter by means of vibroscopy thus demands validation for each type of fibre.

Not only the determination of the fibre geometry but also the fibre's tensile behaviour in a single fibre test need close examination: fibre testing has evolved from the testing of textile fibres and cotton, which show by far lower stiffness than carbon fibres. For instance, Williams and Painter published a comprehensive study of the *pressley cotton fibre strength tester* [16, 17] years before carbon fibres were produced commercially. Furthermore, tensile tests on cotton are often run on fibre bundles instead of single fibres [18, 19]. It should be carefully verified whether methods developed for the cotton industry can be directly transferred to technical fibres (for instance carbon, glass). Whilst several ways to determine the strength of technical fibres are available, common procedures to measure the Young's modulus of fibres have potential for improvement. The pertinent standard mentions direct strain measurements but does not describe procedures how to apply direct measurements of elongation on the fibre, as is common practise for most other types of specimens. Furthermore, the procedure recommended in standard ASTM C1557-14 is time-consuming due to the use of cardboard frames and the need to test various different fibre lengths to account for the systems compliance of the testing device [20]. A correct determination of the system compliance raises an alternative to direct strain measurements. However, the procedure needs to be repeated with different measuring lengths and for different fibres. Most importantly, calculating the systems compliance becomes prone to errors for carbon fibres that exhibit non-linear properties [21, 22]. A detailed examination of today's testing procedures for single fibres was given by the authors of this publication in [23]. As has been shown, only non-contact methods are qualified to be used on single fibres. A common non-contacting method is full-field digital image correlation (DIC), which is widely used to measure displacements and strain in mechanical tests on coupon level and has been the scope of several studies. A comprehensive review is given by Pan *et al* in [24]. A review of Grediac compares digital image correlation with other full-field measurement methods in composite materials [25]. Commonly, a stochastic black-and-white pattern is sprayed on the specimens and imagess taken during the experiment are evaluated with sub-pixel accuracy [25–27]. The implementation in the GOM[1] Aramis software is described in [27]. Digital image correlation procedures on single fibres have also been reported: Hendrickx *et al* and Depuydt *et al* investigated natural fibres and steel wires [28, 29], The authors of the work at hand applied digital image correlation techniques on glass fibres [23]. As demonstrated in a previous work on glass fibres, it is not possible to perform full-field digital image correlation directly on the fibre as images of a fibre do not show a distinct pattern. It is also not expedient to spray a black-and-white pattern on the fibres. Without the ability of applying a stochastic pattern on the fibre, full-field DIC is not feasible in single fibre tensile tests. These problems can be avoided by using polymeric beads as tracking markers

[1] Gesellschaft für optische Messtechnik mbH.

[23]. Instead of using full-field DIC as commonly known for macro-scale specimens, the application of several tracking markers along the fibre allows for optical strain measurements along a single fibre with higher accuracy then indirect strain readings of the testing device would yield. A pairing of two facets in a DIC software is commonly described as 'virtual extensometer', for instance by Ye *et al* [30] comparing full-field DIC, virtual extensometers and optical fibre grating sensors. Instead of using just one virtual extensometer, nine individual 'virtual extensometers' are combined to a linear network of strain measurements in the work at hand.

To run strain measurements on single fibre level, the authors' previous work has used a step-wise procedure to facilitate taking high-resolution images on different load levels. By repeating the load cycle several times, the robustness of the experiment was proven. The beads themselves had no negative influence on the tensile behaviour of the fibre or the testing procedure [23]. This topic will also be addressed briefly in the work at hand.

Given the state-of-the-art in research and technology, it can be deduced that there is a need for improvements in the testing of technical single fibres, such as carbon fibres, by applying direct strain measurements during single fibre tensile tests. As described, common methods of direct strain measurement such as extensometers, strain gauges and full-field DIC cannot be used for testing single fibres. The work at hand transfers DIC-techniques to the field of single fibre testing. It is to some extent built upon methods developed for glass fibers by the authors of this contribution [23].

Accurate measurements of the Young's modulus of carbon fibres are particularly interesting in the light of the fact that high tenacity carbon fibres (HT CF) show a non-linear elastic behaviour. In regions of higher strains, these fibres show increased values for the Young's modulus due to orientations in the crystallite structure [31]. This behaviour has been the scope of several studies: Curtis *et al* [21] investigated the propagation of elastic waves in carbon fibres under various loads and the crystallographic orientation by means of a x-ray microscope. Djordjevic *et al* [32] examined the variations of the Young's modulus of four different carbon fibres in different strain regimes. They applied and discussed linear and square polynomial regressions to correlate the datasets. Kant and Penumadu [22] executed dynamic mechanical tests on single carbon fibres and discussed their non-linear behaviour. They also addressed that compliance corrections of test setups are difficult in case of carbon fibres due to their non-linearity. Shioya *et al* [33] described and modelled the non-linear tensile behaviour of carbon fibres, concluding that a mosaic model was in agreement with mechanical results.

Three specific goals can be derived from the state of the art: firstly, alternative procedures to determine the cross-sectional areas of non-circular carbon fibres are worth exploring. Secondly, investigating the possibilities of direct strain measurement using techniques of digital image correlation are worth evaluating on carbon fibres exhibiting non-linear tensile behaviour. Thirdly, the work at hand addresses the tensile behaviour of recycled and virgin single carbon fibres, improving state-of-the-art testing procedures by fulfilling the need of enhanced and direct strain measurements.

2. Material and methods

2.1. Fibre and recycling

The fibres used in this work are taken from a non-crimp biax fabric of type PANEX35 by Zoltek. In the following, *rCF* will refer to fibres taken directly from pieces of the fabric, thus, they have not been in contact with any resin system. Their single fibre properties can be assumed to be those of virgin (new) fibres. The second material under investigation are recycled fibres, defined as vCF. Here, laminates had been produced by combining the same biax fabric and an epoxy resin in a resin transfer moulding process (RTM) at Fraunhofer ICT[2], Germany. By means of conventional pyrolysis processes at carboNXT GmbH[3], the matrix had been removed.

2.2. Specimen preparation and measuring procedure

The new fibres to be tested were selected from different fibre bundles and the bundles were taken from different areas of the fabric to ensure picking a random sample. Recycled fibres were also taken from different parts of the recycled batch. This procedure shall eliminate measuring errors due to an unintentional selection of neighbouring fibres that might exhibit the same features, for instance in terms of diameter and flaw distribution. However, is has to be mentioned that several of the recycled fibres broke before they could be tested mechanically.

All fibres were tested in a single fibre testing device, SiFiT, which was developed at Karlsruhe Institute of Technology and was described by the authors in a previous work [23].

In reference with figures 1 and 2, the main aspects of the setup and fibre preparation will be highlighted in the following. The experimental setup was installed in a universal testing machine of type Zwick//Roell Z2.5. Instead of using card boards to prepare the fibres, stickers were applied on the fibre as can be seen in figure 1. The upper sticker labeled the fibre and was used to handle the fibre without causing predamages. The fibre was then placed centred between the upper parallel grippers and they were closed with an air pressure of 3 bar. The second, smaller sticker at the bottom end of the fibre served as a weight to align the fibre by gravitational pull. The bottom gripper was then closed and a pretension of 5 mN was applied. This pretension was required to enable correct readings of the diameter and to apply the marker beads without damaging the fibre. When the pretension was applied, the cross-sectional area was determined as will be described in section 2.3. Here, the method applied differs from the procedure published in [23], where diameters of translucent glass fibres were determined optically. Instead, in the work at hand, a laser diffraction sensor was utilised for determining the cross-sectional areas of carbon fibres. Beads were prepared as

[2] www.ict.fraunhofer.de.
[3] www.carbonxt.de/de/home.

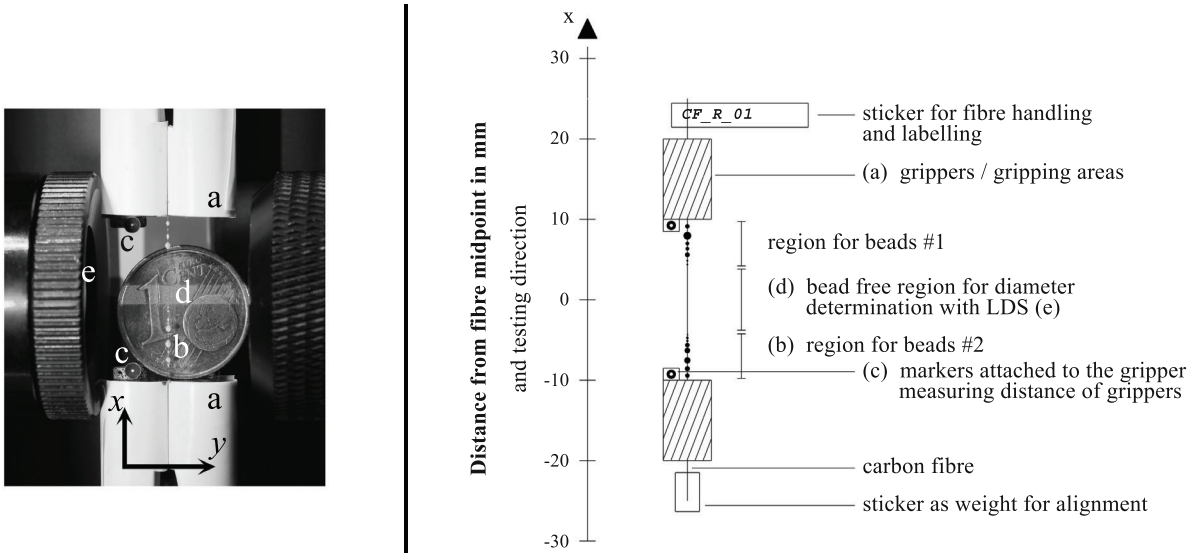

Figure 1. Left: Fibre clamping; the coin is used to visualise the dimensions. Right: Schematic representation of the test setup to emphasise the scale and explain the main parts.

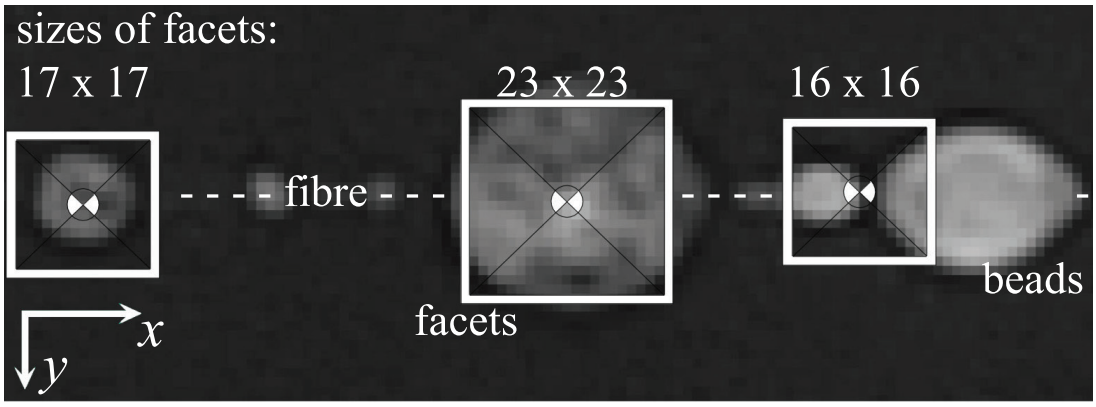

Figure 2. Exemplary facets tacked on the beads in the GOM Aramis software. The square facets were adjusted in size to optimise the software's pattern recognition. They were not necessarily placed on one bead but sometimes between two individual beads if this improved the recognition. Given the fact that the fibre is hardly visible, one can conclude that image correlation can not be run on the fibre itself.

follows: a powder containing orange and yellow fluorescing pigments, ash and carbon powder was mixed. The amounts of these powdery constituents are optimised in order to provide a distinctive optical pattern to be used for digital image correlation in the experiment. A small amount of the powdery mix was blended with a droplet of proformic C1001 by Viko UG glue and then applied onto the fibre. Right after at least five beads were applied in the upper and in the lower region of the measuring length of the fibre, an LED UV light source was used to cure the resin beads within seconds.

After the fibre was properly prepared and its cross-sectional area was measured, the mechanical test was started. In a comparable work on glass fibres, the same authors had applied a step-wise and multiple load cycle to demonstrate the repeatability of the procedure [23]. In the work at hand, the loads are also applied step-wise to take steady images in high-resolutions. Here, the loading cycle is not repeated. Instead, the load is increased in increments Δ_{load} of 250 MPa until final failure of the fibre occurs. In dependence of the tensile strength of the fibres this procedure results in 9 to 25 different load levels and a corresponding number of images. This amendment is beneficial to account for the particularities of high tenacity carbon fibres [22, 32, 33]. The effect of a non-linear increase of the Young's modulus in dependence of the strain region can best be demonstrated when the fibres are loaded until failure. A UV light source was illuminating the beads by fluorescence during the experiment, thereby minimising reflections of the light source. This had been found to be beneficial in terms of experimental robustness [23]. Loads were determined with a XForce HP load cell with a maximum load capacity of 5 N by Zwick//Roell. The loading cycle is depicted in figure 3. Firstly, a pre-cycle is executed. This is to avoid possible fibre slippage during the main experiment. After the pre-cycle the main experiment begins by applying a load of 100 MPa and taking a reference image. Secondly, the load is increased in steps of 250 MPa until final failure. On each load level, an image is taken for subsequent strain measurements in a DIC software.

Given the setup and its constraints, the measuring length of 20 mm corresponds to a length of approximately 2100 pixels,

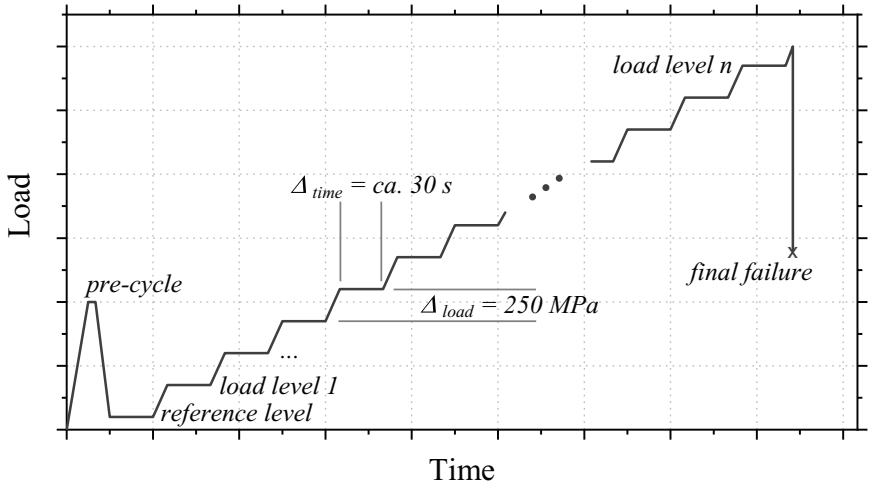

Figure 3. Schematic loading cycle for the single fibre tensile tests. Loads are increased step-wise to allow for gathering of high-resolution images to be post-processed in terms of strain measurements. The pre-cycle is executed to avoid fibre slippage during the experiment and a load level 100 MPa is chosen as reference.

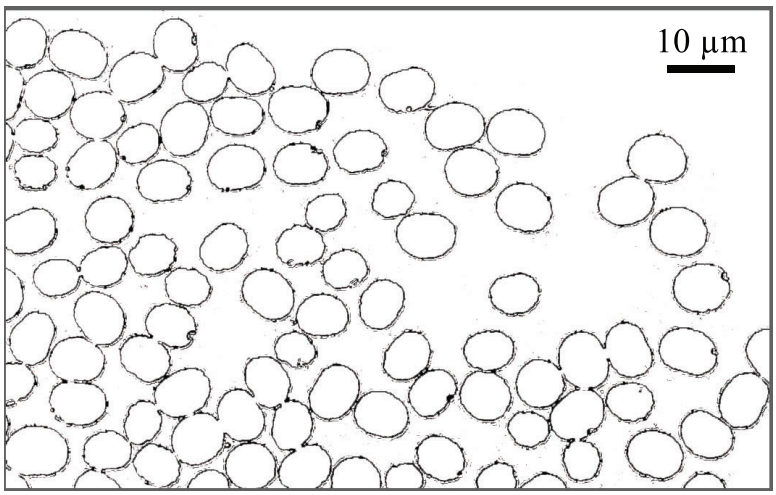

Figure 4. Image of a cross-section of embedded fibres of the same type as used in the single fibre tests. The fibre circumferences are highlighted in black.

or approximately 100 px mm^{-1}. For both fibre populations, virgin and recycled, 13 fibres were validly tested. Results of the mechanical characterisation are described in section 3.2.

2.3. Determination of cross-sectional area

Within the scope of this work, a novel procedure to improve the measurement of the cross-sectional area of carbon fibres was sought. No such procedure has yet been expounded in literature and it expands the state-of-the-art in this field. Therefore, the procedure will be described in detail in this section.

The need for a novel procedure of measuring cross-sectional areas of carbon fibres is illustrated in figure 4. The microsection highlights the circumferences of carbon fibres used in this work embedded in a resin. The carbon fibres show approximately oval cross-sections and the majority of fibres have a convex shape and no indentations. It is thus deduced that conventional methods assuming circular cross-sections are insufficient.

As an accurate determination of the fibre cross-sectional area is essential for correct calculations of the Young's modulus, great care has to be taken when measuring the fibre's cross-sectional area. However, common procedures, for instance vibroscopic measurements, do not take the real fibre shape into account and are based on the assumption of circular cross sections. In this work, an enhanced procedure that considers oval fibre shapes is followed and will be described in this section:

By means of a laser diffraction sensor of type LDS0200 produced by Cersa-mci, 15 individual diameter measurements (D_i') were taken in the middle of the clamping length. The device automatically scans a length of 2 mm along the fibre. The manufacturer guarantees functionality down to diameters of 5 µm but even with smaller diameters an error-free measurement was possible. The laser diffraction sensor was manually rotated about the longitudinal axis of the fibre by the angle ϕ_i in increments of precisely 10°. The measuring principle is schematically shown in figure 5.

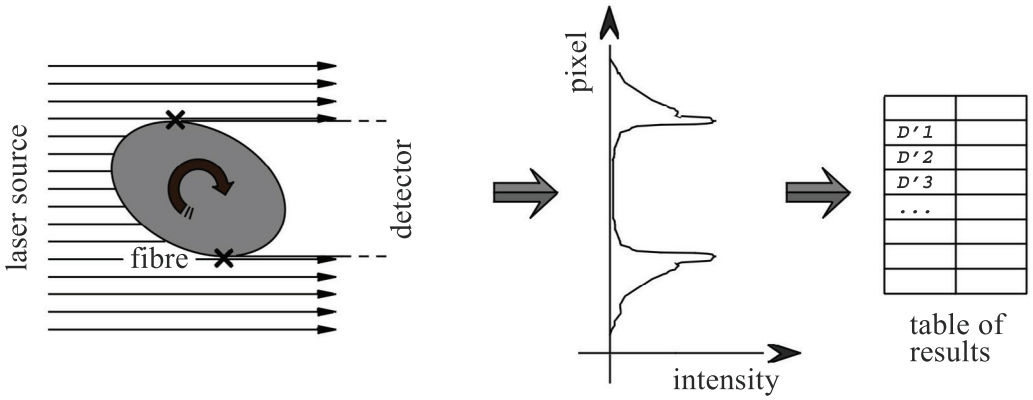

Figure 5. Schematic principal of determining the cross-sectional area by using a laser diffraction sensor.

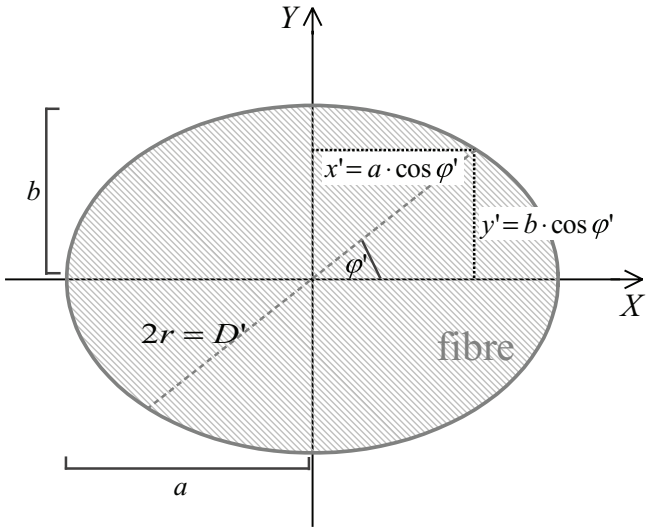

Figure 6. Calculation of cross-sectional area.

The following calculation was used to determine the cross-sectional area and figure 6 gives a graphical description of the geometry.

By applying the equations

$$x' = a \cdot \cos \phi' \tag{2}$$

$$y' = b \cdot \sin \phi' \tag{3}$$

and Pythagoras' theorem

$$(2 \cdot r)^2 = D'^2 = (2 \cdot x')^2 + (2 \cdot y')^2 \tag{4}$$

the half-axes a and b can be determined by

$$D' = \sqrt{(2 \cdot a \cdot \cos \phi')^2 + (2 \cdot b \cdot \sin \phi')^2}. \tag{5}$$

Subsequently, a non-linear fit of least squares is run and yields the maximal and minimal half-axes of the oval. These axes are then used to calculate the area of the oval cross section (A_{fibre}) according to

$$A_{\text{fibre}} = \pi \cdot a \cdot b. \tag{6}$$

Applying the described procedure, slight deviations from a perfect oval are compensated. It also accounts for the missing

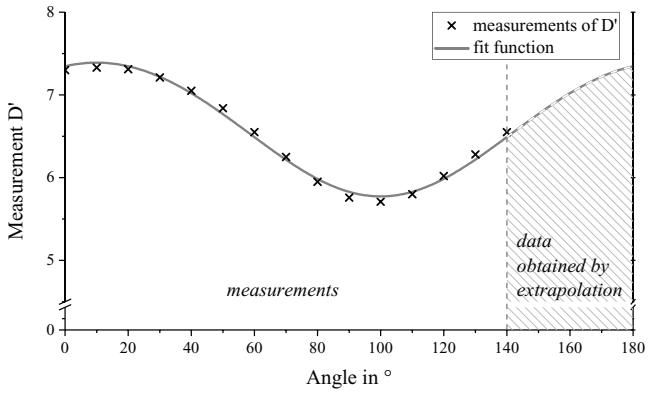

Figure 7. The described fit function applied to the individual measurements D' (represented by **x**) of one of the fibres.

section of 40° which cannot be measured due to constraints given by the dimensions of the setup. The calculation was run for each individual fibre. Reflecting basic geometrical consideration, plotting the readings of the diameter over the angle of rotation will yield a straight line for a perfect circle and a sine-shaped curve for an oval. Thus, the procedure is likewise applicable for oval and circular fibres, as for the latter both half-axes will attain the same value. Exemplary, the data points and the resulting fit are shown in figure 7 for one of the carbon fibres.

The geometrical constraints of the experimental setup did not allow to find the thinnest section along the fibre prior to testing. Thus, the middle-point of the fibre was chosen to determine the cross-sectional area. To demonstrate that within the 20 mm clamping length used in the mechanical test the influence of lengthwise variations of the fibre shape are negligible, five individual, virgin fibres were sequentially clamped with a measuring length of 70 mm. A pre-tension of 10 mN was applied and measurements as described above were taken around the fibre, in this case in steps of 20°. Measurements were repeated in intervals of 5 mm along the fibre and the same fit function was applied to examine if significant variations of the cross-sectional area were apparent in the carbon fibres at use. A total fibre length of 50 mm was evaluated in this experiment, corresponding to 2.5 the length of the fibres in the mechanical tests. The lengthwise continuity of the cross-sectional area of the fibres is graphed in figure 9.

Figure 8. Scheme of pairs of beads evaluated to measure strains directly on the fibre (DSM, facets 1–10) and indirectly on the gripping system (ISM, facets 11–16).

The procedure could not be repeated for recycled fibres as the maximum length of the fibres after recycling was 50 mm, resulting in maximum of 20 mm free measuring length.

2.4. Direct strain measurement and calculation of stiffness

In reference with figure 3, the gathering of data points will be explained in the following. On each of the plateaus an image was taken. Depending on the tensile strength of each individual fibre, this procedure provided different amount of images, with a minimum of 9 images and a maximum 25 images. The following post-processing calculation took place after the experiment: images were opened in the DIC-software GOM Correlate Professional 2017 and on the first frame (reference level), facets were manually applied on the most distinct tracking beads in the software. This was accomplished by maximising the software's pattern quality. As shown schematically in figure 8, a total of 16 facets was used for each fibre.

Facets 1–5 represent the upper region of the fibre, 6–10 the lower region. 11–13 and 14–16 are connected to the gripping system to demonstrate the difference between direct strain measurement (DSM, on the fibre) and indirect measurements (ISM, on the gripping system). Facets 1 and 10 were placed as close as possible to the central axes of the fibre to be used for the alignment of a virtual coordinate system pointing in the positive tensile direction. Digital image correlation was used to track all facets in the series of images for one fibre and a script calculated the strains between the pairs of facets. Firstly, the pairs were taken from the outermost to the innermost beads (1/10, 2/9, etc). Secondly, beads were compared from top to bottom (1/6, 2/7, etc), yielding a total of nine individual strain measurements. Thereby, several benefits could be achieved: faulty or lost facets could be found and replaced. Using nine separate distance measurements in the manner described, heterogeneously distributed strains would be detected. Furthermore, this pairwise evaluation was needed to ensure that the polymer tracking beads do not influence the stiffness of the fibre. The verification that the measuring technique does not have an impact on the results is shown in figure 12. In a previous paper, the authors have also shown by a numerical calculation that the beads have no influence on the fibre properties [23]. Thirdly, the relative change in distance of the grippers was calculated by comparing the pairs 11/16, 12/15 and 13/14. In total, each experimental run provides 12 strain readings per load step and image; nine for DSM and three for ISM to study the differences.

Table 1. Cross-sectional areas of new and recycled fibres.

	Mean cross-sectional area in μm^2	Standard deviation in μm^2	Quantity
Virgin fibres (vCF)	30.99	4.95	260
Recycled fibres (rCF)	30.06	4.93	159

2.5. Scanning electron microscope investigations of fibres and beads

A scanning electron microscope (SEM) of type EVO 50 by Zeiss was used to gain additional information about the fibres' surface character and the tracking beads. Random samples of virgin and recycled fibres and of the beads have been investigated and will be discussed in section 4. In terms of the fibres, SEM was used to access the quality of the fibres surface. Beads were investigated to appraise their quality and connection to the fibre.

3. Results

3.1. Cross-sectional area of fibres

The cross-sectional area was determined according to the procedure presented in section 2.3 for a total of 260 virgin and 159 recycled single carbon fibres randomly picked from different fibre bundles. Thirteen fibres of each population were randomly chosen for tensile tests. Results of the diameter measurement are given as mean values and standard deviation in table 1 for vCF and rCF. No significant difference between virgin and recycled fibres was found. Although the cross-sectional area of the fibres was not reduced due to the pyrolysis process, the recycled fibres are prone to be more fragile when handling them.

As described in section 2.3, the cross-sectional area along the axes of virgin fibre was measured and evaluated. Results for five fibres which were investigated along a measuring length of 50 mm are displayed in figure 9; (a) represents individual measurements for each fibre; (b) their mean values and standard deviations. Whilst the cross-sectional areas of individual fibres differ clearly, only slight variations are found along a fibre. Thus, and for the sake of practicability of single fibre testing, it is acceptable to measure the cross-sectional are a of the fibre in a fixed and central position prior to the mechanical testing process. Given the deviations among

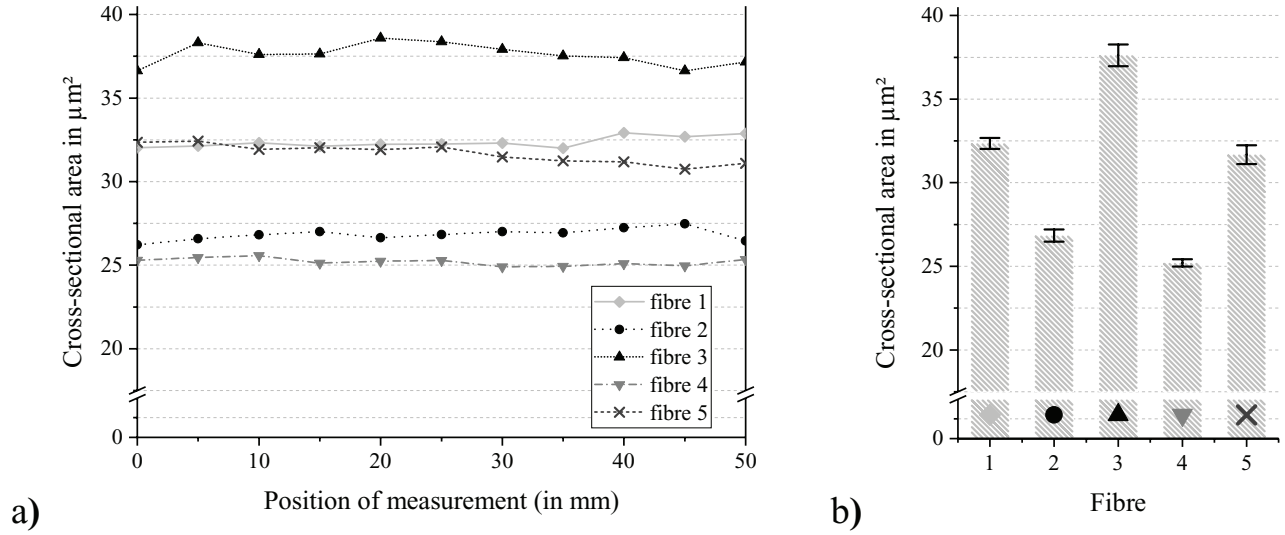

Figure 9. (a) Cross-sectional areas calculated for 11 different positions along the fibre axis; (b) mean values and standard deviations deduced from the individual values as presented in (a).

individual fibres, it is advisable to measure the cross-sectional area of every individual fibre before running mechanical tests instead of calculating with mean values.

3.2. Strain and Young's modulus

According to the procedure described in section 2.4, tensile tests were run. The Young's modulus is calculated and plotted versus the corresponding strain region in figure 10. Virgin fibres (vCF) are displayed as red circles and recycled fibres (rCF) as black crosses. Both will be referred to as direct strain measurements (DSM), as the elongation of the fibre was observed directly. Supplementary, readings obtained by indirect measurements using facets tacked to the gripping system are shown as grey triangles and indicated by ISM. These facets are labelled as 11–16 in figure 8. The grey point clouds only includes measurements gathered simultaneously to the DSM measurements of vCF, but the same effect is seen during the experiments for rCF. One should bear in mind that the displayed variations on single data points in terms of the Young's modulus are a direct consequence of variations in the measurement of the strain and not a property of the fibre itself.

For all point clouds, a linear fit was calculated as proposed by Djordjevic *et al* and Kant and Penumadu [22, 32]. The results of this approximation are listed in table 2.

Compared to the results of virgin fibres, the point cloud of recycled fibres is shifted to lower values of Young's modulus and none of the rCF fibres reaches strains higher than 1.4%. The slopes of the fits are similar. The DSM show a non-linear behaviour, that is, the Young's modulus is higher in regions of higher strains. This non-linearity of high tenacity carbon fibres has been reported before by several authors, as described in section 1. Applying the described step-wise procedure and calculation of the Young's modulus in different strain regions, the non-linearity of carbon fibres can be taken into account appropriately. An extrapolation of the linear fit to 0%-strain shall be used to compare the two different modifications of the carbon fibres: the extrapolation results in a Young's modulus of 300.5 GPa for vCF and 272.5 GPa for rCF, that is a reduction of 9.5% due to the recycling.

Indirect strain measurement result in a Young's modulus of 181.7 GPa, a value well below the expectation.

The figures found for Young's modulus in this work differ significantly from the value stated in the data sheet of the fibres. However, the measuring technique and the strain region are not specified in the data sheet, thus a direct comparison cannot be recommended.

4. Discussion

4.1. Evaluation of cross-sectional area calculation

The procedure presented in this work is optimised to consider oval and circular shapes which are present in the PANEX35 fibres used in this work. Similar fibre shapes are frequently presented in literature, for instance by [5–8, 11]. Given the fibre shapes published by these authors, it can be concluded that the procedure developed here could be used for these types of fibre. To what extent laser diffraction sensors can be applied in investigations of kidney-shaped fibres, as for instance reported in [9, 10], has to be addressed in future work.

Using scanning electron microscopy (SEM) in the work at hand, it was found that recycled fibres show more pronounced grooves along the fibre direction. This change in structure is likely to be a consequence of the pyrolysis process and is exemplary shown in figure 11. Laser diffraction sensors and the calculation procedure used within this work cannot account for these anomalies but will inadvertently smoothen the results and might slightly overestimate the real cross-sectional area. Polymeric beads are shown in the SEM image,

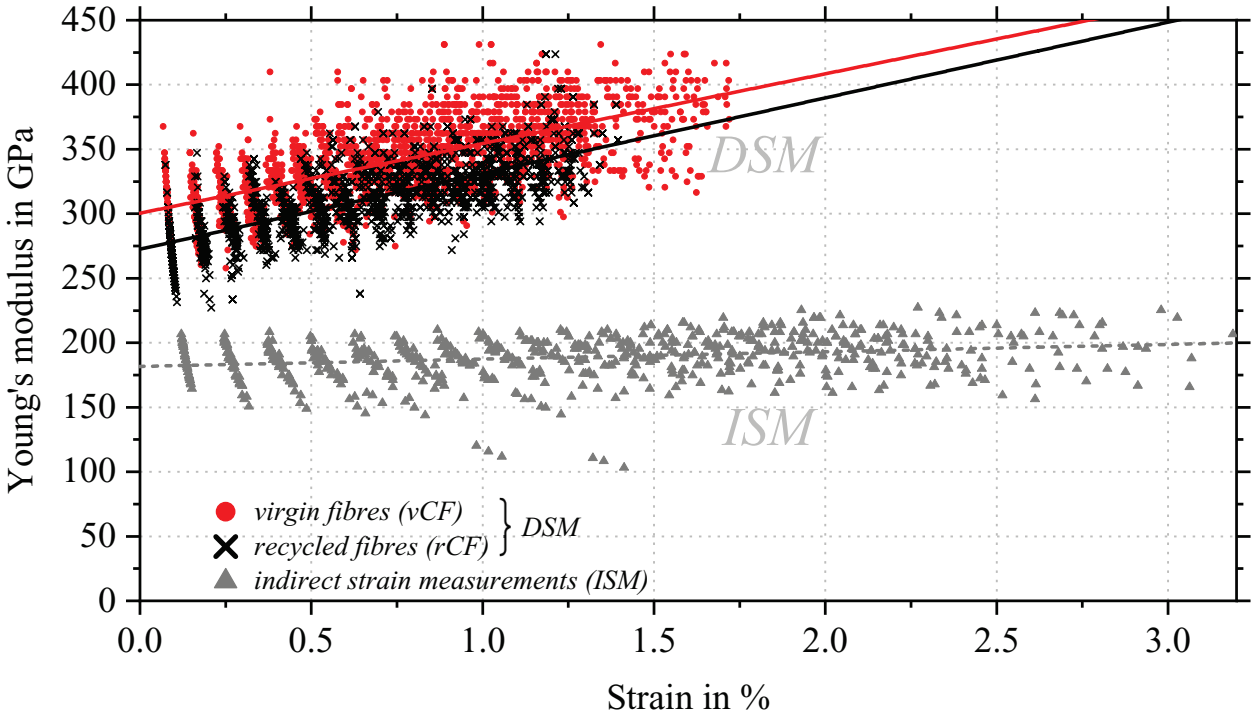

Figure 10. Point clouds of Young's modulus versus strain including every individual direct strain measurement on the single fibre. Red dots represent the virgin fibres, black crosses the recycled fibres and grey triangles show measurements where 'strains' were measured on the gripping system during the experiments for vCF. The lines are linear fits for each of the point clouds. An extrapolation to the *Y*-axis yields the Young's modulus at 0-strain-level. Refer to table 2 for additional information.

Table 2. Intersection and slope of linear fit functions for the direct strain measurements (DSM) on the fibre vCF and rCF and indirect strain measurement (ISM) on the gripping system.

	Virgin fibre	Recycled fibre	ISM
Intersection with *Y*-axes in GPa	300.5 ± 1.0	272.5 ± 1.0	181.7 ± 1.3
Slope in GPa $\%^{-1}$	54.0 ± 1.2	58.6 ± 1.4	5.6 ± 0.9
Pearson correlation coefficient	0.68	0.72	0.25

revealing their characteristic shape, which they obtain due to surface tension.

It is common practice in various mechanical tests to determine the cross-sectional area in the centre of the test specimen. However, measurement errors might be caused by determining the cross-sectional area at the midpoint of the fibre, when slight cross-sectional variations along the fibre are not considered. Nonetheless, the midpoint of the fibre was chosen in order to allow for comparability and practicability. For virgin fibres, it could be demonstrated that the variations of the diameter along the axes of the fibre and within the measuring distance (region of interest) are sufficiently low (see figure 9).

The enhanced method to determine the cross-sectional area approximates the real fibre geometry by assuming an oval structure. This avoids an error described by Titze and Hunter, who reasoned that vibroscopic methods can be falsified if non-circular fibre geometries are not taken into account [14].

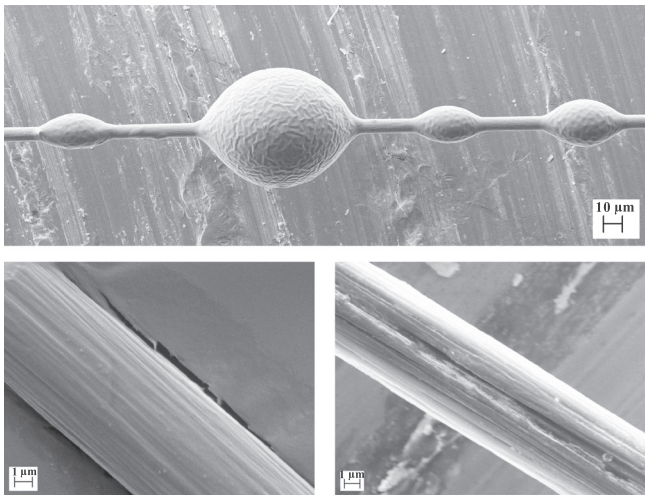

Figure 11. Top: Marker beads applied on a carbon fibre; bottom left: new carbon fibre; bottom right: recycled carbon fibre (pyrolysis) showing pronounced grooves along the fibre direction.

4.2. Additional SEM investigations

As aforementioned, the pyrolysis showed an effect on the fibres. The recycled fibres exhibit a rougher surface in visual examinations (SEM) as shown, for example, in figure 11. Diameters were slightly reduced and, as a consequence, the total mean force to break the fibre was decreased. Nonetheless, the Young's modulus of the recycled and the virgin fibres lie in

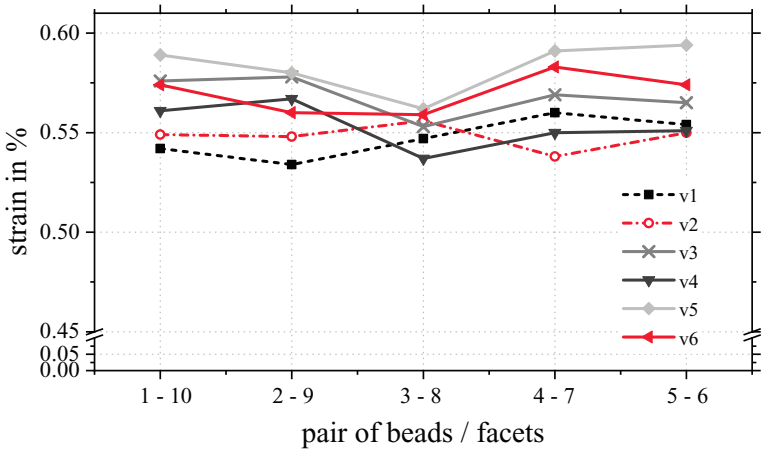

Figure 12. Strain measurements in dependence of the chosen pair of beads. The example shows strain reading measured on the 7th load level for six randomly picked virgin carbon fibres.

Table 3. Validation and accuracy of strain measurements.

	rCF1		rCF2		vCF1		vCF2	
Set value	M	SD	M	SD	M	SD	M	SD
				all in %				
0.5	0.5001	0.0017	0.4992	0.0019	0.5002	0.0028	0.5003	0.0041
1.0	0.9999	0.0032	0.9992	0.0020	1.0002	0.0017	0.9996	0.0038
1.5	1.5013	0.0030	1.4992	0.0025	1.4995	0.0027	1.5005	0.0023
2.0	1.9983	0.0025	1.9997	0.0022	2.0013	0.0032	2.0021	0.0031
2.5	2.5014	0.0022	2.4999	0.0028	2.4999	0.0025	2.5015	0.0022
3.0	3.0005	0.0015	3.0008	0.0021	2.9984	0.0017	2.9997	0.0008
4.0	3.9990	0.0022	3.9997	0.0023	3.9985	0.0022	4.0000	0.0017
5.0	5.0006	0.0025	4.9993	0.0019	4.9970	0.0039	5.0005	0.0027

the same range except. In addition, a SEM image of a series of beads is displayed in figure 11. Due to the surface tension of the polymer, droplet-shaped beads form. Their shape together with features on their surface make them well distinguishable in digital image correlation. As has been shown here and in a previous study [23], these beads do not have an influence on the measurement.

4.3. Discussion of strain deviations

Sixteen facets, ten of them on the fibre, were picked in every initial image. Visual inspections for every image ensured that none of the facets on the fibre was lost during an experimental run. Standard deviations within one set of nine measurements per fibre and per load level were low, rarely exceeding a limit value of 5% relative deviation from the average value. It was deduced that deviations in strain measurement are sufficiently small; variations found in the associated Young's modulus of different fibres are more likely due to physical distinctions of the fibres themselves and not caused by the strain measurement.

The software used for digital image correlation was also capable of tracking deformation of the beads. As the software did not calculate with rigid and squared facets, the midpoint of each facet was not tied to the central pixel of the facet and could move in sub-pixel range.

To demonstrate that it is reasonable to measure strains directly on the fibre, additional measurements were taken between the upper and the lower gripper as indicated in figures 1, 2 and 8. Results are shown in figure 10. These include readings obtained on the gripper (ISM) simultaneously to the experiments with virgin fibres. Results of ISM are presented as the grey point cloud. As can be seen in figure 10, measurements on the gripper significantly overestimate the 'strain[4]', resulting in low values of the Young's modulus. This notable difference is assumed to be caused by the interaction between the fibre and the gripper. In addition to the standard procedure of testing single fibres by glueing them to cardboards [20], the companies Dia-Stron and Textechno offer computer assisted testing systems. In none of these procedures, single fibres are clamped directly by metallic grippers as this would likely cause instant fibre failure upon closing the grippers. Instead, they are embedded in resin or gripped by claws coated with a protective polymer layer. Examples for embedded fibres measured in a LEX820 by Dia-Stron are presented in [34, 35]. Examples of fibre clamping with a fibre-polymer-metal interface when using the automated testing device Favimat + Robot 2 by Textechno, are given in [36, 37].

As a result, an interface between the fibre and the polymeric gripping system is created. There is an unavoidable risk that the fibre slips slightly within the grippers or that the polymeric layer is deformed. Both cause an overestimation

of the 'strain' and consequently a decrease of the 'Young's modulus', as can be clearly comprehended in figure 10. Strain values as high as 3% are found in ISM, obviously surpassing reasonable values for this type of carbon fibres.

As mentioned before, indirect measurements are feasible when the systems compliance is correctly considered and different fibre lengths are tested. However, the non-linearity of carbon fibres raises insecurities of these compensation measurements [21, 22]. The obvious way to reduce this error is to use direct measurements.

The testing procedure raises the question whether the beads applied onto the fibres as tracking markers have themself an influence on the experiment, particularly if they alter the stiffness of the fibre. As has been shown by the same authors in a previous publication [23], this is not the case. Evidence shall also be presented for carbon fibres on the basis of the results obtained in the work at hand. The following example is chosen: six of the vCF were randomly picked and their individual strain readings corresponding to an arbitrary load level, here level 7, of different bead pairs are displayed in figure 12. As described before, pair 1–10 is the outermost, 5–6 the innermost pairing of beads/facets.

If the beads had an influence on the experiment and the fibre stiffness, a clear trend for all fibres would have to emerge here. As can be seen, the individual readings vary randomly and no trend is found. It is concluded that the beads do not affect the measurement.

4.4. Validation and accuracy of strain measurement

In order to prove the accuracy of the 1D DIC testing procedure introduced in this work, the following verification was run. Out of the 13 valid tensile tests for virgin and recycled fibres, two initial images were randomly chosen. These images were graphically distorted in a computer software by factors of 0.5%, 1.0%, 1.5%, 2.0%, 2.5%, 3.0%, 4.0% and 5.0%. Afterwards, the same analysis routine as for the real experiments was run, thus ten facets were positioned in the images and nine individual pairs of facets could be evaluated in terms of strain measurement. Results are listed in table 3.

Standard deviations even at 5.0% elongation are still reasonably low, a value that by far exceeds the possible elongations of carbon fibers. By this verification it is also shown that the DIC software used in this work is capable of processing beads that have been deformed up to 5.0%. Thanks to the unambiguity of the virtual facets, they were not lost even in case of large deformation.

5. Summary and conclusion

A novel procedure to measure strains directly on technical fibres was, for the first time, applied to carbon fibres. The procedure's applicability was demonstrated. In addition, a procedure to approximate the cross-sectional area of carbon fibres which takes into account the non-uniform shape was introduced: instead of assuming circular fibre shapes, the algorithm used in this work can cope with circular and oval shapes equally, the latter being more likely to be found in carbon fibres. Applying both methods, virgin and recycled carbon fibres were compared in terms of their stiffness. The Young's modulus of recycled fibres was reduced by approximately 10% due to the recycling via a pyrolysis route. The fibre surfaces of recycled fibres shows more pronounced grooves along the fibre direction. As aforementioned, single fibre testing could in future be used as a cost-effective alternative method to coupon or full-scale tests when the impact of recycling on fibre composites is under consideration. Demonstrating integrity of carbon fibres after being recycled will give engineers the opportunity to design components containing recycled fibres.

[4] The inverted commas are used to highlight that these values are calculated like a strain and like the Young's modulus but do not represent correct values due to the measurement errors described within this section.

Acknowledgment

This paper is based on investigations of the project *'Verfahrensentwicklung zur Kreislaufführung von Carbonfasern in der Produktion'*, support code MAT0052, of the research program *'Rohstoff- und Materialeffizienz in der Produktion'*. The authors would like to acknowledge the financing by Baden-Württemberg Stiftung gGmbH.

Furthermore, the authors would kindly like to thank Matthias Stoll, Vincent Sessner, Markus Muth, Marc Brecht, Ralf Rössler, Dr Alexander Kauffmann, Pascal Pinter, Miriam Bartkowiak and Anna Trauth for their support and contribution to the work at hand.

ORCID iDs

Jonas Huether https://orcid.org/0000-0002-2129-7400

References

[1] 1999 Directive 99/31/EC of the European Parliament and of the Council on landfill
[2] Pimenta S and Pinho S T 2011 Recycling carbon fibre reinforced polymers for structural applications: technology review and market outlook *Waste Manage.* **31** 378–92
[3] Pimenta S and Pinho S T 2012 The effect of recycling on the mechanical response of carbon fibres and their composites *Compos. Struct.* **94** 3669–84
[4] Granta Design Limited 2016 CES EduPack 2016 (Version: 16.1.22)
[5] Endo M 1988 Structure of mesophase pitch-based carbon fibres *J. Mater. Sci.* **23** 598–605
[6] Chae H G *et al* 2015 High strength and high modulus carbon fibers *Carbon* **93** 81–7
[7] Naito K, Tanaka Y, Yang J-M and Kagawa Y 2008 Tensile properties of ultrahigh strength pan-based, ultrahigh modulus pitch-based and high ductility pitch-based carbon fibers *Carbon* **46** 189–95
[8] Hughes J D H 1986 Strength and modulus of current carbon fibres *Carbon* **24** 551–6
[9] Marcuzzo J S, Otani C, Polidoro H A and Otani S 2013 Influence of thermal treatment on porosity formation on carbon fiber from textile pan *Mater. Res.* **16** 137–44

[10] Kumar S, Anderson D P and Crasto A S 1993 Carbon fibre compressive strength and its dependence on structure and morphology *J. Mater. Sci.* **28** 423–39
[11] Chand S 2000 Review carbon fibers for composites *J. Mater. Sci.* **35** 1303–13
[12] Montgomery D J and Milloway W T 1952 The vibroscopic method for determination of fiber cross-sectional area *Text. Res. J.* **22** 729–35
[13] Bunsell A R 2009 *Handbook of Tensile Properties of Textile and Technical Fibres* (*Woodhead Publishing in Textiles* vol 91) (Oxford: Woodhead Publishing)
[14] Titze I R and Hunter E J 2004 Normal vibration frequencies of the vocal ligament *J. Acoust. Soc. Am.* **115** 2264–9
[15] Lyons K M, Newcomb B A, McDonald K J, Chae H G and Kumar S 2015 Development of single filament testing procedure for polyacrylonitrile precursor and polyacrylonitrile-based carbon fibers *J. Compos. Mater.* **49** 2231–40
[16] Williams S and Painter E 1945 A study of the Pressley cotton fiber strength tester *Text. Res.* **15** 403–12
[17] Pressley E 1942 A cotton fiber strength tester *Am. Soc. Test. Mater. Bull.* **118** 13–7
[18] Barnes J and Elting J 1946 Measurement of cotton fiber strength by the flat taped bundle method *Text. Res. J.* **16** 115–23
[19] ASTM D1445/D1445M-12 2012 *Standard Test Method for Breaking Strength and Elongation of Cotton Fibers (Flat Bundle Method)* (West Conshohocken, PA: ASTM International)
[20] ASTM C1557-14 reaproved 2014 *Standard Test Method for Tensile Strength and Young's Modulus of Fibers* (West Conshohocken, PA: ASTM International)
[21] Curtis G, Milne J and Reynolds W 1968 Non-hookean behaviour of strong carbon fibres *Nature* **220** 1024
[22] Kant M and Penumadu D 2014 Dynamic mechanical characterization for nonlinear behavior of single carbon fibers *Composites* A **66** 201–8
[23] Huether J, Rupp P, Kohlschreiber I and Weidenmann K A 2018 An enhanced method to determine the Young's modulus of technical single fibres by means of high resolution digital image correlation *Meas. Sci. Technol.* **29** 045601
[24] Pan B, Qian K, Xie H and Asundi A 2009 Two-dimensional digital image correlation for in-plane displacement and strain measurement: a review *Meas. Sci. Technol.* **20** 062001
[25] Grediac M 2004 The use of full-field measurement methods in composite material characterization: interest and limitations *Composites* A **35** 751–61
[26] Xavier J, Sousa A M, Morais J J, Filipe V M and Vaz M 2012 Measuring displacement fields by cross-correlation and a differential technique: experimental validation *Opt. Eng.* **51** 043602
[27] Friebe H and Klein M 2016 Optische Bewegungs- und Verformungsanalyse auf Basis applizierter Muster und Marken *5. VDI Fachtagung Optische Messung von Funktionsflächen 2016* pp 47–60
[28] Hendrickx K, Depuydt D, Vuure V, Willem A and Ivens J 2016 The relationship between the tensile properties of natural fibres and their UD composites *Proc. 17th European Conf. on Composite Materials* (MAI Carbon Cluster Management)
[29] Depuydt D, Hendrickx K, Biesmans W, Ivens J and Van Vuure A W 2017 Digital image correlation as a strain measurement technique for fibre tensile tests *Composites* A **99** 76–83
[30] Ye C, Dulieu-Barton J, Webb D, Zhang C, Peng G, Chambers A, Lennard F and Eastop D 2009 Applications of polymer optical fibre grating sensors to condition monitoring of textiles *J. Phys.: Conf. Ser.* **178** 012020
[31] Djordjević I M, Sekulić D R, Mitrić M N and Stevanović M M 2010 Non-Hookean elastic behavior and crystallite orientation in carbon fibers *J. Compos. Mater.* **44** 1717–27
[32] Djordjevic I, Sekulic D and Stevanovic M 2007 Non-linear elastic behavior of carbon fibres of different structural and mechanical characteristic *J. Serb. Chem. Soc.* **72** 513–21
[33] Shioya M, Hayakawa E and Takaku A 1996 Non-Hookean stress-strain response and changes in crystallite orientation of carbon fibres *J. Mater. Sci.* **31** 4521–32
[34] Zhu C, Richardson R M, Potter K D, Koutsomitopoulou A F, van Duijneveldt J S, Vincent S R, Wanasekara N D, Eichhorn S J and Rahatekar S S 2016 High modulus regenerated cellulose fibers spun from a low molecular weight microcrystalline cellulose solution *ACS Sustain. Chem. Eng.* **4** 4545–53
[35] Zhu C, Liu J, Huang S, Rudd C and Liu X 2018 The structure, degradation and fibre drawing properties of phosphate based glasses fibre: the effects of Fe_2O_3 and B_2O_3 addition *CERAM., Silik.* **62** 111–20
[36] Huson M G, Church J S, Kafi A A, Woodhead A L, Khoo J, Kiran M, Bradby J E and Fox B L 2014 Heterogeneity of carbon fibre *Carbon* **68** 240–9
[37] Foulk J A and Mcalister D D III 2002 Single cotton fiber properties of low, ideal, and high micronaire values *Text. Res. J.* **72** 885–91